Characteristics of In(Ga)As quantum ring infrared photodetectors

H. S. Ling, S. Y. Wang, C. P. Lee, and M. C. Lo

Citation: Journal of Applied Physics **105**, 034504 (2009); doi: 10.1063/1.3075836
View online: http://dx.doi.org/10.1063/1.3075836
View Table of Contents: http://scitation.aip.org/content/aip/journal/jap/105/3?ver=pdfcov
Published by the AIP Publishing

Characteristics of In(Ga)As quantum ring infrared photodetectors

H. S. Ling,[1] S. Y. Wang,[2] C. P. Lee,[1] and M. C. Lo[1]
[1]*Department of Electronic Engineering, National Chiao Tung University, 1001 Ta Hsueh Road, Hsinchu 300, Taiwan*
[2]*Institute of Astronomy and Astrophysics, Academia Sinica, P.O. Box 23-141, Taipei, Taiwan*

(Received 30 September 2008; accepted 21 December 2008; published online 3 February 2009)

Characteristics of In(Ga)As quantum ring infrared photodetectors (QRIPs) were investigated under normal incidence configuration. Compared with quantum dot infrared photodetectors (QDIPs), QRIPs showed wider photocurrent spectra, more stable responsivity with temperature change, and lower dark current activation energy. The wide detection band comes from the transitions from the quantum ring (QR) ground states to different excited states. The shallow confinement states generate higher dark current and enhance the carrier flow between the QRs within the same QR layer. This carrier flow averages out the repulsive potential and makes QRIPs behave similarly to the quantum well infrared photodetectors instead of QDIPs. With an $Al_{0.27}Ga_{0.73}As$ current blocking layer, the performance of QRIPs was greatly enhanced. © *2009 American Institute of Physics*.
[DOI: 10.1063/1.3075836]

I. INTRODUCTION

Infrared photodetectors based on intraband transitions in III-V materials are of great potential to be economical alternatives to the present leading HgCdTe based interband detectors. With this motivation, quantum well infrared photodetectors (QWIPs) and quantum dot infrared photodetectors (QDIPs), especially for the *n*-type devices, were widely studied with different spectral ranges in past decades.[1–13] With the intersubband transitions, the fractional spectral widths ($\Delta\lambda/\lambda$) of the photocurrent spectra are usually smaller than 30% in both QWIPs and QDIPs. However, these two kinds of detectors possess distinct characteristics because of the differing quantum confinement in their structures. In quantum wells (QWs), the electrons are confined within the potential wells in the vertical direction but are free to move along the wells. As a result, QWIPs are only sensitive to radiations with the electric field polarized perpendicular to the QWs. The current conductive gain of QWIPs is usually low and quite stable at different temperatures.[1] In contrast, with the three-dimensional quantum confinement for the active media, QDIPs exhibit strong in-plane polarized photoresponse,[12,13] much higher current gain, and strong temperature dependence of responsivity.[5] With the advances in nanostructure growth, it is expected that new structures with different confinement schemes will generate detectors with different properties. Recently, quantum rings (QRs) were used as the absorption media in infrared detectors and the response spectra showed a wide fractional spectral widths ($\Delta\lambda/\lambda$) larger than 60%.[14] By exploiting the much shallower bound-state energies of the QR structure,[15,16] Dai *et al.*[17] demonstrated that it is easy to extend the detection band into the terahertz regime. Quantum ring infrared photodetectors (QRIPs), therefore, provide a new approach for the long wavelength broadband infrared detection. However, the detailed characterization for QRIPs and their optimization have not been reported so far, and the reported performance is still much worse than those of QWIPs and QDIPs.

In this paper, the detailed characteristics of In(Ga)As/GaAs QRIPs were investigated and compared with those of QWIPs and QDIPs. Although the physical distribution of QRs is discrete and similar to those of quantum dots (QDs), the closely separated shallow bound states of QRs make the device perform differently from QDIPs but rather similarly to QWIPs. With a proper design and the use of an AlGaAs current blocking layer, the performance of QRIPs is greatly enhanced.

II. BASIC CHARACTERISTICS OF THE SAMPLE

The sample used in this study was grown by a Veeco GEN-II molecular beam epitaxy system on a (001) semi-insulating GaAs substrate. Thirty layers of In(Ga)As QRs separated by 50 nm GaAs barrier layers were grown as the active region with n^+ GaAs contact layers on both sides. A 75 nm $Al_{0.27}Ga_{0.73}As$ layer was added on top of the bottom contact layer as the current blocking layer. An additional surface QR layer was also deposited for the atomic force microscopy (AFM) measurement. The growth procedure of the QRs began with 2.8 monolayers (MLs) of InAs QDs covered with 2 nm of GaAs layer. Twelve second growth interruption was followed for the formation of QRs. Finally, a high growth rate GaAs layer was deposited to minimize the deformation of the as grown ring structures. A Si δ-doped layer with a concentration of 5×10^9 cm^{-2} was inserted 2 nm under each QR layer. Figure 1(a) shows the AFM image of the surface QRs. QRs with uniform sizes are clearly observed with a density around 1.8×10^{10} cm^{-2}. The average outer and inner diameters are about 60 and 15 nm, and the height is around 2–3 nm. The structure of the imbedded QRs was also confirmed with cross-sectional transmission electron microscopy, as shown in Fig. 1(b). The lateral and vertical dimensions of the imbedded QRs are very close to the AFM result obtained from QRs on the surface. The high growth rate of the capping layer effectively preserved the morphology of QRs.

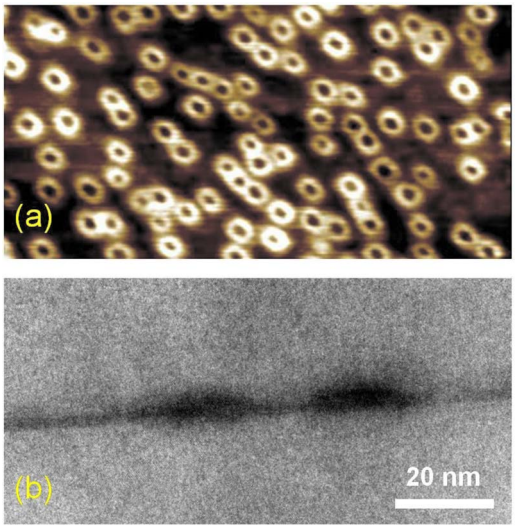

FIG. 1. (Color online) (a) 1×0.5 μm^2 AFM image of the surface QRs. (b) The cross-sectional TEM image of a single QR.

The sample was then examined with the photoluminescence (PL) spectroscopy to probe the electron energy states in the QRs. Figure 2 shows the 77 K PL spectra with two different excitation powers. The ground state energy of the sample is 1.238 eV. Due to the reduced height of the QRs, the ground state energy is much higher than the ground state energy of QDs with the same nominal InAs thickness.[16] The shape of the low power spectrum is very close to a Gaussian function with a full width at half maximum (FWHM) of 43 meV, indicating the single size distribution of the QRs. Under high excitation power, four excited states and one wetting layer (WL) state were revealed. The transition energies of these excited states are at 1.290, 1.325, 1.364, and 1.40 eV, respectively. Compared with QDs, the spacing between the energy levels, however, are reduced due to the larger lateral extent of the rings.

Discrete devices were fabricated by standard processing techniques. 260×370 μm^2 mesas with AuGe contact rings were formed to allow normal incidence measurement from the mesa top. The sample was mounted on the cold finger of a close cycled helium cryostat for the photocurrent measurements at different temperatures. For all measurements, the bottom contact was referred as ground.

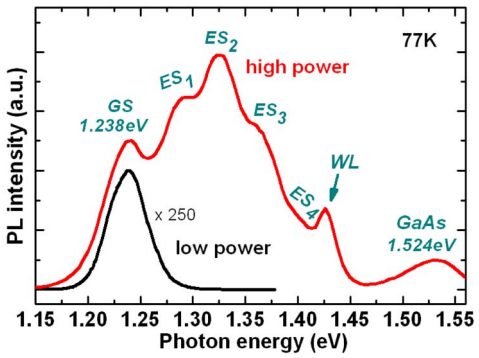

FIG. 2. (Color online) The PL spectra of the sample at 77 K with different excitation powers. The excited state peaks are indicated in the high excitation spectrum.

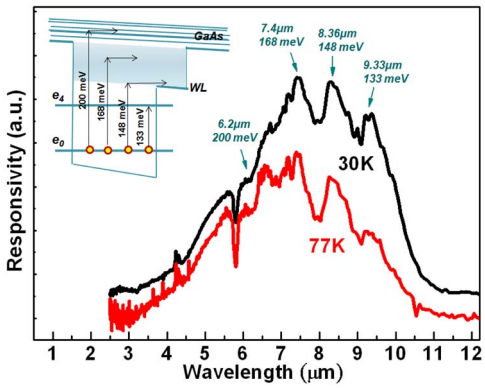

FIG. 3. (Color online) The responsivity spectra of the sample at 30 and 77 K. The inset shows the transitions associated with the responsivity peaks.

III. RESULTS AND DISCUSSIONS

The photocurrent spectra were obtained with a Nicolet 550 Fourier transform infrared spectrometer under normal incidence configuration. Figure 3 shows the response spectra at 30 and 77 K. Although QRIPs are expected to be less sensitive to the normal incident radiation due to the flattened geometry of QRs, the normal incident signal is still strong and clear. The polarization dependent response was further examined with the 45° edge-coupling scheme. The TE (*E*-field polarized in the QR plane) to TM (*E*-field polarized in the growth direction) response ratio of the sample is about 11%. This number, although smaller than that in QDIPs, is still stronger than that in QWIPs.

The responsivity spectrum shows a broadband detection with the center wavelength around 8 μm and a bandwidth of 5 μm ($\Delta\lambda/\lambda\sim60\%$). Unlike the single peak usually seen in QWIPs or QDIPs, multiple peaks were seen in the spectrum. From the AFM image and the PL spectrum, the QRs are quite uniform in size, indicating that the wide detection band is not from the multimodal distribution of the QRs. Instead, the multipeak spectrum is caused by the transitions of electrons from the QR ground state to different excited states including QR bound states, WL states, and GaAs continuum states. It is known that the GaAs band gap at 77 K is 1.507 eV,[18] and the WL transition energy determined by the high power PL spectrum is 1.426 eV. Assuming a 7:3 ratio for the conduction/valence band discontinuity at the heterointerface and with a given ground state energy of 1.238 eV, any radiation with the photon energy higher than 188 meV will be able to excite electrons in a QR to the GaAs barrier. The broad peak around 6.2 μm (200 meV) is thus from the transition from the ground state to the GaAs continuum states. The two response peaks at 7.4 and 8.36 μm correspond to the transitions from the ground state to the WL states. Finally, the lowest energy peak at 9.33 μm is from the transition to the fourth QR excited state. The above four excitation schemes are also schematically plotted in the inset of Fig. 3. It might be suspected that some of the response peaks are from the first excited states to the higher states. However, those transitions will have energy lower than the peaks detected. Furthermore, the doping density used in our sample is much lower than the QR density, and the probability for electrons to populate the excited states is quite low. Finally,

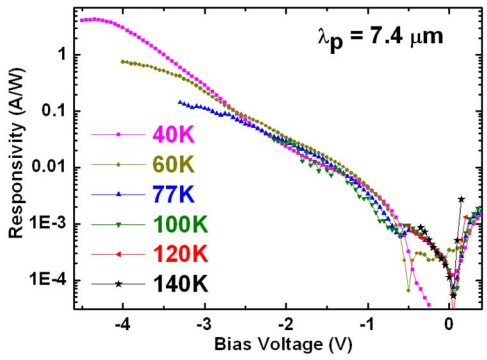

FIG. 4. (Color online) The voltage dependence of the peak responsivity of the sample at different temperatures.

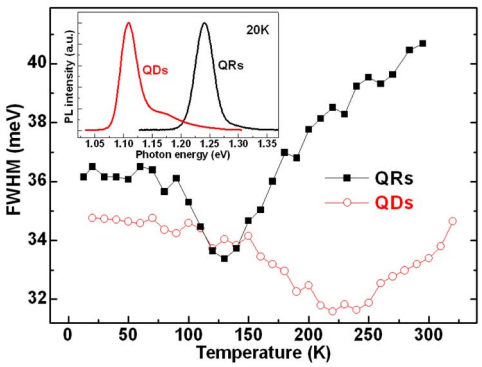

FIG. 5. (Color online) Temperature dependent FWHM of the PL spectra of single-layer QRs (solid symbol) and single-layer QDs (unfilled symbol). The inset shows their spectra at 20 K.

given that no obvious change in the response spectra at different bias levels was detected, we conclude that the responsivity peaks are unlikely to have originated from the excited states.

On the other hand, for the QDIPs with the same 2.8 ML InAs QDs as in the QRIP sample, only the signal associated with the WL transition was observed.[5] The quantum states in QRs are weakly confined, and the state energies are closer to the GaAs band edge when compared with the quantum states in QDs. The ground state electron wave function extends further outside of the QR region and enhances the bound to continuum transitions in QRIPs. Due to the higher states energy with respect to the GaAs band edge, the escape probability for the transition to the QR fourth excited states is much higher in QRs. The deep bound states in QDs prohibit the generation of photocurrent from such transitions.

It is also evident in Fig. 3 that the responsivity spectra at 30 and 77 K are slightly different at longer wavelength. The long wavelength peaks (8.36 and 9.33 μm) decrease from 30 to 77 K while other peaks remain at the same level. As mentioned, the carriers excited to the lower energy states need more energy to escape from potential trap before being trapped back to the ground states. At higher temperatures, it was found that the excited electrons are more likely to be trapped in the QRs than to contribute to the photocurrent.[19] Due to the lower excited state energy, this effect is more severe for the 9.33 μm peak, and it decays more than the 8.36 μm peak from 30 to 77 K.

The absolute responsivity was then calibrated by a 1000 °C blackbody radiation source with a Ge wafer inserted in the optical path to block the photocurrent caused by interband excitations. Lock-in technique was used with the chopper frequency set at 1 kHz. Due to the inserted AlGaAs layer, the responsivity is quite weak under positive biases so the following discussions are limited to the negative biases only. The peak responsivity at different negative biases and temperatures are plotted in Fig. 4. The responsivity is quite stable from 40 to 100 K for a wide bias range (-2.8–-0.6 V). This phenomenon is different from that in QDIPs, in which the responsivity usually increases over a decade in this temperature range. For QDIPs, the dramatic increase in responsivity with temperature is due to the rapid increase in current gain, which is the result of the repulsive coulomb potential caused by the extra carriers inside the QDs.[5] For QRIPs, however, the repopulation of carriers is faster within individual QR layer because of the higher ground state energy. Thus, the current gain and therefore the responsivity are more stable against temperature variation. This temperature stability is similar to that of QWIPs in which carriers flow freely in the QW plane. The fast carrier flow and the large lateral extent of the QRs with higher ground state energy also increase the probability for the conductive free carriers being captured into the QRs. The current gain of our QRIP sample at -1 V and 77 K is only 0.003, which is much lower than that measured under the same conditions in QDIPs with a similar device structure. The carrier flow within the QR plane and the high capture probability of free carriers make QRIPs behave like QWIPs in the transport characteristics.

To verify the difference of the carrier flow within a QR and a QD layer, two samples, each with a single layer of QDs or QRs, were prepared. The same amount of InAs was used in both samples but the QR sample had an additional partially capping and annealing process for the ring formation. The carrier flow information could be extracted by examining the temperature dependent PL linewidth variation.[20] The PL spectra of the two samples and their FWHM as functions of temperature are compared in Fig. 5. As expected, the ground state energy for the QRs is higher than that of the QDs for more than 100 meV. The widths of the PL spectra of the two samples both decreased first and then broadened with the increase in temperature. At extremely low temperatures, the width of the PL signal is from the nonequilibrium and random distribution of carriers in QRs or QDs, and is usually wider. With the increase in temperature, the carrier distribution will be closer to the quasiequilibrium condition with a common Fermi level for the whole ensemble. The temperature with minimum spectral width indicates that, above this temperature (T_m), the thermal energy is high enough for carriers to flow freely between the QRs or QDs. For the QD sample, T_m was found to be around 230 K. But, for the QR sample, the linewidth shrank much faster and T_m occurred at 130 K. Such a large difference in T_m indicates that electrons within a QR layer can move more freely to repopulate the QRs. The facilitated carrier repopulation in the QR layer makes the current gain and the responsivity in QRIPs insensitive to the temperature change.

The dark current of the device was also measured at

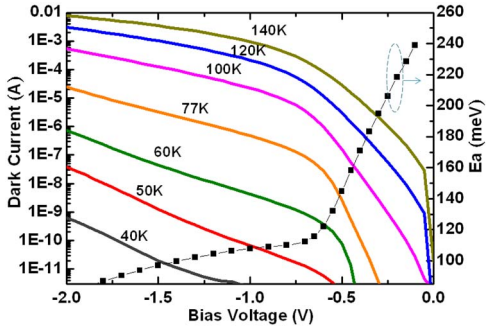

FIG. 6. (Color online) The voltage dependence of the dark current of the sample with different temperatures and the dark current activation energies (E_a) at different bias voltages.

different temperatures with a helium dewar. The measured dark current curves and the extracted activation energy (E_a) are shown in Fig. 6. The E_a shown here was calculated assuming $I_d \propto T \exp(-E_a/kT)$. Both the dark current and E_a exhibit two distinct regions in the figure. E_a drops dramatically at a lower bias region but then decreases with a lower slope when the bias is over −0.65 V. Accordingly, the dark current curves also show two different increasing rates with biases for the temperatures higher than 60 K. By extrapolation, the zero bias E_a was estimated to be in the range of 250–260 meV, which agrees well with the conduction band discontinuity of the $Al_{0.27}Ga_{0.73}As/GaAs$ heterointerface [256 meV (Ref. 18)]. It means that the voltage drop is essentially on the $Al_{0.27}Ga_{0.73}As$ layer from 0 to −0.65 V and the dark current is limited by the wide band gap material. When the bias further increases, the applied voltage starts to drop on the active region, and E_a is then dominated by the effective Fermi level in the QR layer. In this domain, the activation energy at −0.7 V was 112 meV, which is close to the reported activation energy for the QRIP without the AlGaAs barrier.[14] Such small activation energy in QRIPs prohibits the high temperature operation and is the result of the higher ground state energy. Hence, the adoption of a wide band gap layer in QRIPs is necessary for the operation at elevated temperatures.

The noise current spectra of the device were measured by feeding the amplified dark current signal into a fast Fourier transform spectrum analyzer. The noise current density at 1 kHz was then used to calculate the specific detectivity. The detectivity measured at 77 K and −1 V is 2.8×10^8 cm $Hz^{0.5}/W$ for normal incident devices and is 8.1×10^8 cm $Hz^{0.5}/W$ for 45° coupled devices. At 140 K, the highest detectivity measured for the QRIP was 1.2×10^8 cm $Hz^{0.5}/W$ at −0.1 V for 45° devices. In this regime, the dark current was highly suppressed by the AlGaAs layer so the performance of the QRIP could be measured up to 140 K. It should be mentioned that the device performance measured here is based on the normal incident configuration without any grating couplers. The device performance can be enhanced with a properly designed grating coupler.

The characteristics of In(Ga)As QRIPs were investigated. The thinner InAs thickness and wider extent of the QR structure generated higher but closer electron state energies, and weaker wave function confinement. This induces the specific features of QRIPs such as wider photocurrent spectra, more stable responsivity with temperature change, and lower dark current activation energy. The broad spectral response comes from the transitions of electrons from the QR ground state to the QR excited bound states, the WL states, and the GaAs continuum states. The higher confinement state energy and the extended wave function in QRIPs induce better carrier flow within each QR layer as well as lower current gain. Such behaviors make QRIPs have similar transport properties with QWIPs instead of QDIPs. For high temperature operation of QRIPs, wide band gap layer should be inserted into the devices to compensate for the inherently small ionization energy of carriers. The performance of long wavelength QRIPs was greatly enhanced with an $Al_{0.27}Ga_{0.73}As$ current blocking layer.

[1] B. F. Levine, J. Appl. Phys. **74**, R1 (1993).
[2] A. D. Stiff, S. Krishna, P. Bhattacharya, and S. W. Kennerly, IEEE J. Quantum Electron. **37**, 1412 (2001).
[3] H. Lim, S. Tsao, W. Zhang, and M. Razeghia, Appl. Phys. Lett. **90**, 131112 (2007).
[4] S. Chakrabarti, A. D. Stiff-Roberts, P. Bhattacharya, S. Gunapala, S. Bandara, S. B. Rafol, and S. W. Kennerly, IEEE Photonics Technol. Lett. **16**, 1361 (2004).
[5] S. Y. Wang, M. C. Lo, H. Y. Hsiao, H. S. Ling, and C. P. Lee, Infrared Phys. Technol. **50**, 166 (2007).
[6] S. Y. Wang, S. D. Lin, H. W. Wu, and C. P. Lee, Infrared Phys. Technol. **42**, 473 (2001).
[7] P. Aivaliotis, L. R. Wilson, E. A. Zibik, J. W. Cockburn, M. J. Steer, and H. Y. Liu, Appl. Phys. Lett. **91**, 013503 (2007).
[8] H. S. Ling, S. Y. Wang, C. P. Lee, and M. C. Lo, Appl. Phys. Lett. **92**, 193506 (2008).
[9] E. T. Kim, A. Madhukar, Z. Ye, and J. C. Campbell, Appl. Phys. Lett. **84**, 3277 (2004).
[10] D. Pal, L. Chen, and E. Towe, Appl. Phys. Lett. **83**, 4634 (2003).
[11] D. Pan, E. Towe, and S. Kennerly, Appl. Phys. Lett. **73**, 1937 (1998).
[12] L. Chu, A. Zrenner, G. Bohm, and G. Abstreiter, Appl. Phys. Lett. **75**, 3599 (1999).
[13] S. D. Chen, Y. Y. Chen, and S. C. Lee, Appl. Phys. Lett. **86**, 253104 (2005).
[14] J. H. Dai, Y. L. Lin, and S. C. Lee, IEEE Photonics Technol. Lett. **19**, 1511 (2007).
[15] H. Pettersson, R. J. Warburton, A. Lorke, K. Karrai, J. P. Kotthaus, J. M. Garcia, and P. M. Petroff, Physica E **6**, 510 (2000).
[16] H. S. Ling and C. P. Lee, J. Appl. Phys. **102**, 024314 (2007).
[17] J. H. Dai, J. H. Lee, Y. L. Lin, and S. C. Lee, Jpn. J. Appl. Phys. **47**, 2924 (2008).
[18] I. Vurgaftman, J. R. Meyer, and L. R. Ram-Mohan, J. Appl. Phys. **89**, 5815 (2001).
[19] H. Lim, W. Zhang, S. Tsao, T. Sills, J. Szafraniec, K. Mi, B. Movaghar, and M. Razeghi, Phys. Rev. B **72**, 085332 (2005).
[20] C. Lobo, R. Leon, S. Marcinkevicius, W. Yang, P. C. Sercel, X. Z. Liao, J. Zou, and D. J. H. Cockayne, Phys. Rev. B **60**, 16647 (1999).